Time-dependent Gutzwiller theory of magnetic excitations in the Hubbard model

G. Seibold,[1] F. Becca,[2] P. Rubin,[3] and J. Lorenzana[4]
[1]*Institut für Physik, BTU Cottbus, P.O. Box 101344, 03013 Cottbus, Germany*
[2]*INFM-Democritos, National Simulation Centre, and SISSA I-34014 Trieste, Italy*
[3]*Institute of Physics, University of Tartu, Riia 142, 51014 Tartu, Estonia*
[4]*Center for Statistical Mechanics and Complexity, INFM, Dipartimento di Fisica, Università di Roma La Sapienza, Piazzale Aldo Moro 2, 00185 Roma, Italy*

(Received 6 November 2003; revised manuscript received 26 January 2004; published 26 April 2004)

We use a spin-rotational invariant Gutzwiller energy functional to compute random-phase-approximation-like (RPA) fluctuations on top of the Gutzwiller approximation (GA). The method can be viewed as an extension of the previously developed GA+RPA approach for the charge sector [G. Seibold and J. Lorenzana, Phys. Rev. Lett. **86**, 2605 (2001)] with respect to the inclusion of the magnetic excitations. Unlike the charge case, no assumptions about the time evolution of the double occupancy are needed in this case. Interestingly, in a spin-rotational invariant system, we find the correct degeneracy between triplet excitations, showing the consistency of both computations. Since no restrictions are imposed on the symmetry of the underlying saddle-point solution, our approach is suitable for the evaluation of the magnetic susceptibility and dynamical structure factor in strongly correlated inhomogeneous systems. We present a detailed study of the quality of our approach by comparing with exact diagonalization results and show its much higher accuracy compared to the conventional Hartree-Fock+RPA theory. In infinite dimensions, where the GA becomes exact for the Gutzwiller variational energy, we evaluate ferromagnetic and antiferromagnetic instabilities from the transverse magnetic susceptibility. The resulting phase diagram is in complete agreement with previous variational computations.

DOI: 10.1103/PhysRevB.69.155113 PACS number(s): 71.10.−w, 71.27.+a, 71.45.Gm

I. INTRODUCTION

It is now about 40 years ago that Gutzwiller proposed a variational wave function for correlated electronic models with a purely local interaction, i.e., for the Hubbard-like models.[1,2] The basic idea is to partially project out configurations with doubly occupied sites from the Fermi sea in order to optimize the contributions from kinetic and potential energy. As a consequence, in contrast to the conventional Hartree-Fock (HF) theory, the Gutzwiller wave function captures correlation effects such as the band narrowing already on the variational level. However, the exact evaluation of the ground-state energy within the Gutzwiller wave function is fairly difficult and up to now has only been achieved in one and infinite dimensions.[3] In the latter case the solution is equivalent to the so-called Gutzwiller approximation (GA) which has been applied to describe a variety of finite-dimensional systems ranging from the properties of normal ^{3}He (see Ref. 4) to the stripe phase of high-T_c cuprates.[5,6]

The GA in its original formulation was restricted to homogeneous paramagnetic systems and only later on generalized to arbitrary Slater determinants by Gebhard[7] and, more recently, by Attaccalite and Fabrizio.[8] The same energy functional was obtained from the Kotliar-Ruckenstein (KR) slave-boson formulation of the Hubbard model when the bosons are replaced by their mean values.[9] Moreover, the KR slave-boson approach provides a controlled scheme for including fluctuations beyond the mean-field solution. Formally this has been achieved by several authors within the functional integral formalism.[10–14] However, the expansion of the KR hopping factor z^{SB} turned out to be a highly nontrivial task, both with respect to the proper normal ordering of the bosons and with respect to the correct continuum limit of the functional integral.[10] These difficulties have severely hampered the computation of charge fluctuations within the slave boson approach. To our knowledge this technique has therefore only been applied to *toy models*[10] and to compute the optical conductivity in the paramagnetic regime.[13,14] The latter, however, did not lead to controlled sum rules due to the above mentioned difficulties.[15]

In Refs. 16,17 we have developed an alternative scheme for the computation of random-phase-approximation-like (RPA) fluctuations beyond the GA. Our approach, labeled GA+RPA, is based on well-developed techniques in nuclear physics[18] and RPA fluctuations are obtained in the small oscillation limit of a time-dependent GA. By comparing with exact diagonalization results, we have shown that the computation of static and dynamical correlation functions performs much better within the GA+RPA than within conventional HF+RPA theory.[19] Since no restrictions are imposed on the symmetry of the saddle-point solution, the GA+RPA method is also suitable for the investigation of strongly correlated electronically inhomogeneous systems. Based on this formalism, two of us have recently explained the evolution of the optical conductivity with doping in high-T_c cuprate compounds.[20]

Our previous investigations were restricted to the evaluation of RPA fluctuations in the charge sector where the z component of the spin is conserved by the particle-hole excitations.[16,17] However, in general, one has to distinguish between longitudinal (i.e., with $\Delta S_z=0$) and transverse spin excitations (i.e., with $\Delta S_z=\pm 1$), the latter involving particle-hole pairs with opposite spins. Longitudinal excitations are optically allowed by dipole selection rules whereas

transverse excitations can be excited by spin-carrying particles such as neutrons. For spin-rotational invariant systems, the triplet transverse excitations with $\Delta S_z = \pm 1$ are degenerate with the triplet longitudinal excitation with $\Delta S_z = 0$ and, therefore, it is enough to solve the problem in the longitudinal channel. As discussed below, the solution in the transverse channel is useful for a consistency check. If spin-rotational symmetry is broken, (e.g., for ferromagnetic or spin-density-wave states) the triplet excitations will split and one has to solve both channels to obtain the whole spectrum.

The present paper is therefore devoted to the computation of transverse magnetic excitations on top of the GA. Various approaches have been already adopted in order to accomplish this task. In Ref. 21, Bünemann has evaluated the spin-wave excitations in itinerant ferromagnets by determining variationally the energy of the excited state $S_q^+|\Psi_G\rangle$, where $|\Psi_G\rangle$ denotes the Gutzwiller wave function and S_q^+ is the spin-flip operator with momentum q. Furthermore, spin excitations around paramagnetic saddle points have been investigated in Refs. 11,12,22 within the functional integral technique based on the spin-rotational invariant slave-boson scheme.[23]

Our investigations below are related to these previous investigations but differ in two important aspects. First we will eliminate the bosonic degrees of freedom (except for the double occupancy D) from the energy functional, which thus only depends on the density matrix and the parameters D. Formally, this procedure defines an effective Gutzwiller Hamiltonian, which can be expanded with respect to both charge and spin fluctuations. As usual, both types of excitations are decoupled in case of saddle points with collinear spin structure. Second, the density matrix can be constructed from arbitrary Slater determinants, and, therefore, the method is suitable for the investigation of magnetic excitations in inhomogeneous systems. In this respect, the size limitations in numerical solutions are exactly the same than for the inhomogeneous HF+RPA approach.[19]

The paper is organized as follows. In Sec. II we derive the GA energy functional from the spin-rotational invariant slave-boson Hamiltonian and show how RPA fluctuations in the charge and spin channel can be obtained within the time-dependent Gutzwiller approach. In particular, we focus on the magnetic excitation spectrum obtained in this way from the Hubbard model. Results for specific systems are presented in Sec. III. As a first example, we consider in Sec. III A the two-site Hubbard model, where the analytical solution is available for comparison. Since at small U the mean-field ground state is spin-rotationally invariant, the expected degeneracy between longitudinal and transverse spin excitation allows us to check the consistency among charge and magnetic channel computations. Then, in Sec. III B, the method is applied to a homogeneous and paramagnetic GA solution, where it turns out that the evaluation of transverse magnetic susceptibilities is greatly simplified as compared to previous approaches. In particular, we evaluate the ferromagnetic and antiferromagnetic instability lines for an infinite-dimensional hypercubic system, and demonstrate the exact agreement with variational results. Section III C is devoted to a comparison of the GA+RPA magnetic excitation spectra with exact diagonalization and HF+RPA results, respectively. Concluding remarks appear in Sec. IV.

II. FORMALISM

A. Spin-rotational invariant GA

The starting point is the one-band Hubbard model:

$$H = \sum_{i,j,\sigma} t_{ij} c_{i,\sigma}^{\dagger} c_{j,\sigma} + U \sum_i n_{i,\uparrow} n_{i,\downarrow}, \tag{1}$$

where $c_{i,\sigma}$ ($c_{i,\sigma}^{\dagger}$) destroys (creates) an electron with spin σ at site i, and $n_{i,\sigma} = c_{i,\sigma}^{\dagger} c_{i,\sigma}$. U is the on-site Hubbard repulsion and t_{ij} denotes the hopping parameter between sites i and j. Our investigations are based on the spin-rotational invariant form of the slave-boson approach introduced by KR.[23] Within this formalism one introduces auxiliary bosons e_i ($e_i^{\dagger}$) and d_i ($d_i^{\dagger}$) which represent the annihilation (creation) of empty and doubly occupied sites, respectively. In addition, the singly occupied states are represented by two particles, a spin-1/2 fermion and a boson p which can have either spin $S=0$ or $S=1$ in such a way that the combination has spin-1/2. The four p states (a singlet and a triplet) are combinations of the elements $p_{i,\sigma\sigma'}$ of a 2×2 matrix $\mathbf{p}_i$. In the saddle-point approximation all boson operators are treated as numbers and the matrix $\mathbf{p}_i$ can be parametrized as

$$\mathbf{p}_i = \begin{pmatrix} p_{i,\uparrow} & \frac{1}{\sqrt{2}} p_i \exp(-i\phi_i) \\ \frac{1}{\sqrt{2}} p_i \exp(+i\phi_i) & p_{i,\downarrow} \end{pmatrix}, \tag{2}$$

with p_i, $p_{i\sigma}$, and ϕ_i real.

Besides the completeness condition

$$e_i^2 + \mathrm{tr}(\mathbf{p}_i^* \mathbf{p}_i) + D_i = 1, \tag{3}$$

the boson fields are constrained by the following relations

$$\mathrm{tr}(\boldsymbol{\tau}_\mu \mathbf{p}_i^* \mathbf{p}_i) + 2\,\delta_{\mu,0} D_i = \sum_{\sigma,\sigma'} (\boldsymbol{\tau}_\mu)_{\sigma,\sigma'} \rho_{ii}^{\sigma,\sigma'}, \tag{4}$$

where, in general, $\rho_{ij}^{\sigma,\sigma'} \equiv \langle c_{i,\sigma}^{\dagger} c_{j,\sigma'} \rangle$ denotes the density matrix, $\boldsymbol{\tau}_\mu$ are the Pauli matrices (including $\boldsymbol{\tau}_0 \equiv \mathbf{1}$), and $D_i \equiv d_i^2$.

After rewriting the Hamiltonian (1) in terms of fermion and boson operators,[23] we can construct a *spin-rotational invariant Gutzwiller functional* by eliminating the boson fields except for D_i via the constraints, Eqs. (3) and (4). As a result, one obtains

$$E^{GA} = \sum_{i,j,\sigma,\sigma_1,\sigma_2} t_{ij} z_{i,\sigma_1,\sigma} z_{j,\sigma,\sigma_2} \rho_{ij}^{\sigma_1,\sigma_2} + U \sum_i D_i, \tag{5}$$

where the matrix $\mathbf{z}_i$ reads as

$$\mathbf{z}_i = \begin{pmatrix} z_i^+ \cos^2\frac{\Phi}{2} + z_i^- \sin^2\frac{\Phi}{2} & \frac{S_i^-}{S_i^z}[z_i^+ - z_i^-]\cos\Phi \\ \frac{S_i^+}{S_i^z}[z_i^+ - z_i^-]\cos\Phi & z_i^+ \sin^2\frac{\Phi}{2} + z_i^- \cos^2\frac{\Phi}{2} \end{pmatrix}, \tag{6}$$

with

$$\tan^2\Phi = \frac{S_i^+ S_i^-}{(S_i^z)^2}, \tag{7}$$

$$z_i^\pm = \frac{\sqrt{1-\rho_{ii}+D_i}\lambda_i^\pm + \lambda_i^\mp\sqrt{D_i}}{\sqrt{(1-D_i-(\lambda_i^\pm)^2)(\rho_{ii}-D_i-(\lambda_i^\mp)^2)}}, \tag{8}$$

$$(\lambda_i^\pm)^2 = \rho_{ii}/2 - D_i \pm S_i^z\sqrt{1+\tan^2\Phi}, \tag{9}$$

and for clarity spin expectation values are denoted by $S_i^+ = \rho_{ii}^{\uparrow,\downarrow}$, $S_i^- = \rho_{ii}^{\downarrow,\uparrow}$, $S_i^z = (\rho_{ii}^{\uparrow,\uparrow} - \rho_{ii}^{\downarrow,\downarrow})/2$, and $\rho_{ii} = \rho_{ii}^{\uparrow,\uparrow} + \rho_{ii}^{\downarrow,\downarrow}$. Note that in the limit $S_i^\pm = 0$, where the matrix $\mathbf{z}_i$ is diagonal, one recovers the standard Gutzwiller energy functional as derived by Gebhard[7] or KR.[9] Furthermore, it has been shown that the spin-rotational invariant slave-boson scheme can be derived from the KR (or alternatively Gebhard's) energy functional when the spin rotation is applied to the underlying Slater determinant.[24] Therefore, Eq. (5) can be viewed as the more general GA-like energy functional for a Hubbard Hamiltonian.

In order to obtain the stationary solution of Eq. (5) one has to minimize E^{GA} with respect to the double occupancy parameters D and the density matrix ρ. The latter variation has to be constrained to the subspace of Slater determinants by imposing the condition

$$\rho^2 = \rho, \tag{10}$$

which is equivalent to the diagonalization of the electronic problem supplemented by the variation with respect to D only. A detailed description of the corresponding formalism can be found in Ref. 25.

Regarding the stationary solutions, we will restrict to Slater determinants which are diagonal in spin space, i.e., $\rho_{ij}^{\sigma,\sigma'(0)} = \rho_{ij}^{\sigma,\sigma(0)}\delta_{\sigma,\sigma'}$. Thus we do not consider spin canted solutions[26] which would mix charge and spin excitations. The diagonalized density matrices have eigenvalue 1 below the Fermi level ($\equiv$ hole states: h) and zero above ($\equiv$ particle states: p) and consequently are also diagonal in spin space:

$$\rho_{h\sigma,h\sigma}^{(0)} = 1, \tag{11}$$

$$\rho_{p\sigma,p\sigma}^{(0)} = 0. \tag{12}$$

Within this notation we can formally write the stationary GA energy as

$$E^{GA} = \sum_{k\sigma} \epsilon_k \rho_{k\sigma,k\sigma}^{(0)} + U\sum_i D_i^{(0)}, \tag{13}$$

where the superscript "(0)" indicates quantities evaluated in the stationary state, $k = p,h$ labels particle and hole states, and ϵ_k are the corresponding one-particle energies.

B. Calculation of RPA fluctuations around general GA saddle points and magnetic excitations

The energy functional Eq. (5) is a convenient starting point for the calculation of charge and spin excitations on top of general GA wave functions. In Refs. 16,17, we have already given a detailed derivation of the GA+RPA formalism in the charge sector, which, in the following, we extend to include the spin fluctuations.

We thus study the response of the system to an external time-dependent perturbation

$$F(t) = \sum_{i,j,\sigma,\sigma'} [f_{ij,\sigma\sigma'}(t) c_{i,\sigma}^\dagger c_{j,\sigma'} + \text{H.c.}], \tag{14}$$

$$f_{ij,\sigma\sigma'}(t) = f_{ij,\sigma\sigma'}(0) e^{-i\omega t}, \tag{15}$$

which induces small amplitude oscillations of D and ρ around the GA saddle point

$$D = D_i^{(0)} + \delta D(t), \tag{16}$$

$$\rho = \rho^{(0)} + \delta\rho(t). \tag{17}$$

Correspondingly, we have to expand the energy functional Eq. (5) around the stationary solution up to second order in the density and double-occupancy deviations. Due to the fact that we restrict to collinear saddle-point solutions, the charge and spin sectors in the expansion are decoupled and one obtains

$$E[\rho,D] = E_0 + \text{tr}(h^0\delta\rho) + \delta E^{charge} + \delta E^{spin}, \tag{18}$$

where we have introduced the Gutzwiller Hamiltonian:[27,28]

$$h_{ij}^{\sigma,\sigma'}[\rho,D] = \frac{\partial E^{GA}}{\partial \rho_{ji}^{\sigma',\sigma}}\delta_{\sigma,\sigma'}. \tag{19}$$

δE^{charge} contains the expansion with respect to the double-occupancy parameters and the part of the density matrix, which is diagonal in the spin indices. This part of the RPA problem has already been studied in detail in Refs. 16,17, where it was shown that the δD fluctuations can be eliminated by assuming that they adjust instantaneously to the evolution of the density matrix (antiadiabaticity condition).

The spin part of the expansion reads

$$\delta E^{spin} = \sum_{i,j,\sigma} t_{ij}\rho_{ij}^{(0)\sigma,\sigma}[z_{i,\sigma,\sigma}^{0}\delta_2 z_{j,\sigma,\sigma} + z_{j,\sigma,\sigma}^{0}\delta_2 z_{i,\sigma,\sigma}]$$
$$+ \sum_{i,j,\sigma} t_{ij} z_{i,\sigma,\sigma}^{0}[\delta_1 z_{j,\sigma,-\sigma}\delta\rho_{ij}^{\sigma,-\sigma}$$
$$+ \delta_1 z_{j,-\sigma,\sigma}\delta\rho_{ji}^{-\sigma,\sigma}]$$
$$+ \sum_{i,j,\sigma} t_{ij}\rho_{ij}^{(0)\sigma,\sigma}\delta_1 z_{i,\sigma,-\sigma}\delta_1 z_{j,-\sigma,\sigma}, \quad (20)$$

with the following abbreviations for the quadratic parts of the z-factor expansion

$$\delta_1 z_{i,\sigma,-\sigma} = \frac{\partial z_{i,\sigma,-\sigma}}{\partial \rho_{ii}^{-\sigma,\sigma}}\delta\rho_{ii}^{-\sigma,\sigma}, \quad (21)$$

$$\delta_2 z_{i,\sigma,\sigma} = \frac{\partial^2 z_{i,\sigma,\sigma}}{\partial \rho_{ii}^{\sigma,-\sigma}\partial \rho_{ii}^{-\sigma,\sigma}}\delta\rho_{ii}^{\sigma,-\sigma}\delta\rho_{ii}^{-\sigma,\sigma}. \quad (22)$$

The explicit results for the derivatives are given in Appendix A. It is interesting to observe that, in contrast to the charge excitations, the evaluation of the magnetic excitations can be performed without any adjustment of δD to $\delta\rho$, i.e., without any assumption on the time evolution of D. Only in the case of noncollinear saddle points one would have a coupling between spin and charge fluctuations and, therefore, the necessity to invoke the antiadiabaticity condition to eliminate the δD deviations.

The density fluctuations $\delta\rho$ in the expansion Eq. (18) are restricted to the subspace of Slater determinants, i.e., they have to obey the constraint Eq. (10). One can therefore divide $\delta\rho$ into the particle (p) and hole (h) sectors using the property of the density matrices Eqs. (11) and (12):

$$\{\delta\rho_{\sigma\sigma'}^{hp}\} \equiv \rho_{\sigma\sigma}^{(0)}\delta\rho(1-\rho_{\sigma'\sigma'}^{(0)}), \quad (23)$$

$$\{\delta\rho_{\sigma\sigma'}^{ph}\} \equiv (1-\rho_{\sigma\sigma}^{(0)})\delta\rho\rho_{\sigma'\sigma'}^{(0)}, \quad (24)$$

$$\{\delta\rho_{\sigma\sigma'}^{hh'}\} \equiv \rho_{\sigma\sigma}^{(0)}\delta\rho(1-\rho_{\sigma'\sigma'}^{(0)}), \quad (25)$$

$$\{\delta\rho_{\sigma\sigma'}^{pp'}\} \equiv (1-\rho_{\sigma\sigma}^{(0)})\delta\rho\rho_{\sigma'\sigma'}^{(0)}. \quad (26)$$

where by $\{\delta\rho_{\sigma\sigma'}^{hp}\}$ we mean a matrix whose nonzero generic elements are of the form $\delta\rho_{\sigma\sigma'}^{hp}$. Moreover, one can show [see Eqs. (34)–(36) in Ref. 17] that the pp and hh density projections yield a quadratic contribution in the ph and hp matrix elements in the small amplitude approximation

$$\delta\rho_{\sigma\sigma'}^{hh} \approx -\sum_{p\sigma''}\delta\rho_{\sigma\sigma''}^{hp}\delta\rho_{\sigma''\sigma'}^{ph}, \quad (27)$$

$$\delta\rho_{\sigma\sigma'}^{pp} \approx \sum_{h\sigma''}\delta\rho_{\sigma\sigma''}^{ph}\delta\rho_{\sigma''\sigma'}^{hp}. \quad (28)$$

Hence, although the Gutzwiller Hamiltonian Eq. (19) is diagonal in spin space, it turns out that the term $\mathrm{tr}(h^0\delta\rho) = \Sigma_\mu \epsilon_\mu \rho_{\mu\mu}$ in Eq. (18) (which is first order in the pp and hh density projections) yields a quadratic contribution in the ph and hp matrix elements:

$$\mathrm{tr}(h^0\delta\rho) = \sum_{p\sigma}\epsilon_p\delta\rho_{\sigma\sigma}^{pp} + \sum_{h\sigma}\epsilon_h\delta\rho_{\sigma\sigma}^{hh},$$
$$= \sum_{ph\sigma\sigma'}(\epsilon_p - \epsilon_h)\delta\rho_{\sigma\sigma'}^{ph}\delta\rho_{\sigma'\sigma}^{hp}. \quad (29)$$

The fluctuations which are diagonal in the spin indices ($\delta\rho_{\sigma\sigma}^{ph}$ and $\delta\rho_{\sigma\sigma}^{hp}$) contribute to the expansion in the charge channel,[17] whereas the nondiagonal elements describe the zero-order (noninteracting) spin-flip excitations of the saddle-point Slater determinant.

Thus, up to second order in the particle-hole (spin) density fluctuations, one obtains for the energy expansion

$$\delta E^{spin} = \frac{1}{2}(\delta\rho^{hp}, \delta\rho^{ph})\begin{pmatrix} A & B \\ B^* & A^* \end{pmatrix}\begin{pmatrix} \delta\rho^{p'h'} \\ \delta\rho^{h'p'} \end{pmatrix}, \quad (30)$$

where the explicit expressions for the RPA matrices A and B are given in Appendix B. Note that the shorthand notation in Eq. (30) and below implies that p and h states have opposite spin, i.e., $\delta\rho^{ph}$ represent the joint set of elements of types $\delta\rho_{\uparrow\downarrow}^{ph}$ and $\delta\rho_{\downarrow\uparrow}^{ph}$. Following Ref. 17, we can now evaluate the response function corresponding to the perturbation Eq. (14). In case of nondiagonal perturbations (as the coupling to a current), one has to define an associated Gutzwiller operator which contains the GA hopping matrices $\mathbf{z}_i$. However, in the spin channel the most relevant perturbations couple an external field locally to some spin operator. The field $f_{ij,\sigma\sigma'} = f_{ii,\sigma\sigma'}\delta_{ij}$ is therefore diagonal in the site representation and remains unchanged within the GA. Upon transforming the perturbation to the particle-hole representation one can derive the following linear response equation:

$$\left\{\begin{pmatrix} A & B \\ B^* & A^* \end{pmatrix} - \hbar\omega\begin{pmatrix} 1 & 0 \\ 0 & -1 \end{pmatrix}\right\}\begin{pmatrix} \delta\rho^{ph} \\ \delta\rho^{hp} \end{pmatrix} = -\begin{pmatrix} f_{ph} \\ f_{hp} \end{pmatrix}. \quad (31)$$

The inversion of Eq. (31) yields a linear relation between the external field and the change in the density

$$\delta\rho = R(\omega)f, \quad (32)$$

and defines the linear response function $R(\omega)$ which in the Lehmann representation reads as

$$R(\omega)_{ph,p'h'} = \sum_{n>0}\left[\frac{X_{ph}^n X_{p'h'}^{n*}}{\omega - \Omega_n + i\epsilon} - \frac{Y_{p'h'}^n Y_{ph}^{n*}}{\omega + \Omega_n + i\epsilon}\right], \quad (33)$$

where we have introduced the eigenvectors of the RPA matrix

$$\langle 0|a_h^\dagger a_p|n\rangle \equiv X_{ph}^n, \quad (34)$$

$$\langle 0|a_p^\dagger a_h|n\rangle \equiv Y_{hp}^n. \quad (35)$$

and $|n\rangle$ denote the unprojected (i.e., without Gutzwiller correlations) excited states of the RPA problem.

III. RESULTS

The RPA formalism derived in the preceding section constitutes a convenient starting point for the calculation of spin excitations on top of the GA. One of the advantages of the present approach is that it is suitable for general Slater determinants, i.e., without any restriction on translational and (longitudinal) spin symmetries. The system sizes[29] which can be treated are the same than for the traditional HF+RPA approximation.[19] However, also for homogeneous and paramagnetic saddle points the GA based RPA approach provides a convenient method for the evaluation of spin fluctuations. Our method is solely based on the expansion of the density matrix in terms of particle-hole fluctuations and does not involve other degrees of freedom as in the related functional integral slave-boson scheme.[11,12,22]

First, this advantage is demonstrated for a two-site Hubbard model which is also a convenient *toy model* for the RPA formalism derived in the preceding section. However, the GA+RPA approach can also be applied within the more conventional Green's function technique which is used in Sec. III B to evaluate spin susceptibilities for a homogeneous and paramagnetic hypercubic lattice in infinite dimensions. In this case the GA becomes exact for the energy functional within the Gutzwiller wave function, and we recover the magnetic instability lines determined previously by Fazekas and collaborators.[30] The remainder of this section is then devoted to a detailed analysis of the quality of our approach by comparing with HF+RPA and exact results for small clusters, where the exact solution is known by exact diagonalization techniques.

A. Two-site Hubbard model

As a first example, we consider the two-site Hubbard model at half filling which can be solved exactly and can be studied analytically with both the GA+RPA and HF+RPA approximations. On general grounds a mean-field (or time-dependent mean-field) approach is expected to improve as the dimensionality of the space increases, and, therefore, this zero-dimensional problem is the worst case and may give an estimation of the maximum error which can be expected for these mean-field approaches.

The exact ground-state energy is given by

$$E_0 = \tfrac{1}{2}[U - \sqrt{U^2 + 16t^2}], \tag{36}$$

and only the antisymmetric combination of the spin-flip operators

$$S^{\pm}_{\pi} = \frac{1}{\sqrt{2}}[S^{\pm}_1 - S^{\pm}_2] \tag{37}$$

induces a transition to a state with energy $E=0$, so that the excitation energy is given by $\omega^{ex}_{spin} = -E_0$.

Note that the exact solution does not display a phase transition but remains paramagnetic (and analytic) in U/t. On the other hand, in the HF theory, one finds a paramagnetic solution below $U^{HF}_{crit}/t = 2$ and a Néel-type ordered solution for $U > U^{HF}_{crit}$. The latter is clearly nonphysical and related to the mentioned limitation of mean-field in a low-dimensional system. In the GA approximation, the electronic correlations are approximated in a better way and the range of the paramagnetic solution is extended, giving rise to

$$U^{GA}_{crit}/t = 8(\sqrt{2}-1) \approx 3.31$$

Since the analytic expressions for the symmetry-broken regime become quite lengthy, we restrict the derivation below to the paramagnetic case, where the expansion of the energy functional is given by

$$\delta E^{spin} = \frac{4U_s}{N} \sum_{q=0,\pi} \delta S^{+}_{q} \delta S^{-}_{-q},$$

$$U^s = -u\frac{(2+u)(1-u)}{1+u}t, \quad u = U/(8t).$$

Note that within the HF+RPA approximation, we have $U^s = -U/4$.

The RPA matrices read as

$$A = \begin{pmatrix} \Delta E + 2U^s & 0 \\ 0 & \Delta E + 2U^s \end{pmatrix}, \quad B = \begin{pmatrix} 0 & 2U^s \\ 2U^s & 0 \end{pmatrix},$$

with the one-particle excitation energies $\Delta E = 2t(1-u^2)$.

The diagonalization of the eigenvalue problem yields two degenerate excitation energies

$$\omega^2_{\lambda=1,2} \equiv \Omega^2 = \Delta E[\Delta E + 4U^s]. \tag{38}$$

Since the ground state is a singlet, these energies in the spin channel coincide with the longitudinal magnetic excitations computed in the charge channel (see Ref. 17). Correspondingly, one has three triplet excitations in total, with $\Delta S_z = -1,0,1$. This indicates that the spin-rotation invariance is correctly implemented in our approach, a fact that is far from being trivial. It is worth noting that in the charge channel an extra assumption was needed, namely, the antiadiabatic adjustment of the double occupancy to the time evolution of the density matrix, which was not necessary for the present calculation. Therefore, the fact that the spin-rotation symmetry is preserved among both independent computations can be used as a justification *a posteriori* of the previous assumption.

B. Paramagnetic regime in infinite dimensions

As a further application and to get more insight into our approximation, we apply the GA+RPA method to an infinite-dimensional hypercubic lattice, where the performance is expected to be the best. We consider a partially filled system with density $n = 1-\delta$.

The on-site elements of the density matrix for a paramagnetic saddle-point solution are given by $\rho^{\sigma,\sigma'}_{ii} = n/2\,\delta_{\sigma\sigma'}$, so that the matrix $\mathbf{z}_i$ of Eq. (6) reads as

$$\mathbf{z}_i = \begin{pmatrix} z_0 & 0 \\ 0 & z_0 \end{pmatrix}, \tag{39}$$

where, by using the notation introduced by Vollhardt in Ref. 4, we have

$$z_0 = \sqrt{\frac{2x^2 - x^4 - \delta^2}{1-\delta^2}}, \tag{40}$$

$$x = \sqrt{1-n+D} + \sqrt{D}. \tag{41}$$

For the Gutzwiller approximated energy one obtains

$$E^{GA} = N z_0^2 e_0 + NUD, \tag{42}$$

$$z_0^2 e_0 = \frac{1}{N} \sum_{k\sigma} \varepsilon_k \rho_{kk}^{\sigma,\sigma}, \tag{43}$$

where e_0 denotes the energy per site of the noninteracting system, ε_k is the electronic dispersion corresponding to the Gutzwiller Hamiltonian (19) and N is the number of sites. The minimization of Eq. (42) yields

$$\frac{x^4(1-x^2)}{x^4-\delta^2} = (1-\delta^2)\frac{U}{8|e_0|} \equiv u, \tag{44}$$

which, by using Eq. (41), determines the double-occupancy parameter D.

The energy expansion Eq. (20) in the momentum space is given by

$$\delta E^{spin} = \frac{1}{N} \sum N_q \delta S_q^+ \delta S_{-q}^- + \frac{1}{N} \frac{z'}{z_0} \times \sum_q (\delta T_q^+ \delta S_{-q}^- + \delta S_q^+ \delta T_{-q}^-), \tag{45}$$

with the following definitions:

$$N_q = 2 e_0 z_0 z'' + \left(\frac{z'}{z_0}\right)^2 \frac{1}{N} \sum_{k\sigma} \varepsilon_{k+q} \rho_{kk}^{\sigma,\sigma}, \tag{46}$$

$$\delta S_q^\sigma = \sum_k \delta \rho_{k+q,k}^{\sigma,-\sigma}, \tag{47}$$

$$\delta T_q^\sigma = \sum_k (\varepsilon_{k\pm q} + \varepsilon_k) \delta \rho_{k+q,k}^{\sigma,-\sigma}, \tag{48}$$

and the derivatives z' and z'' are given in Appendix A.

Within the RPA approach presented in Sec. II, one always computes all excitation energies, which constitutes a suitable procedure for the solutions on finite clusters. In infinite system it is usually more convenient to treat the RPA problem in terms of a conventional Dyson approach. Therefore, we use the well-known equivalence between both formulations[19] to set up a Dyson equation. The interaction kernel which enters the S matrix in the Green's function description can be formally obtained from Eq. (45) by substituting the density-matrix fluctuations by the corresponding operator expressions, for instance

$$\delta S_q^+ \to S_q^+ = \sum_k c_{k+q,\uparrow}^\dagger c_{k,\downarrow},$$

$$\delta T_q^+ \to T_q^+ = \sum_k (\varepsilon_{k+q} + \varepsilon_k) c_{k+q,\uparrow}^\dagger c_{k,\downarrow}.$$

Since the energy expansion Eq. (45) is a quadratic form in $\delta S_q^\pm$ and $\delta T_q^\pm$ it is useful to define the following matrix for the bare time-ordered correlation functions

$$\boldsymbol{\chi}_q^0(t) = \frac{i}{N} \begin{pmatrix} \langle \mathcal{T} S_q^+(t) S_{-q}^-(0)\rangle_0 & \langle \mathcal{T} S_q^+(t) T_{-q}^-(0)\rangle_0 \\ \langle \mathcal{T} T_q^+(t) S_{-q}^-(0)\rangle_0 & \langle \mathcal{T} T_q^+(t) T_{-q}^-(0)\rangle_0 \end{pmatrix}, \tag{49}$$

where, the notation $\langle \cdots \rangle_0$ indicates that the correlation functions are calculated from the excitation spectrum of the Gutzwiller Hamiltonian Eq. (19) and (29) and as a function of frequency one obtains

$$\boldsymbol{\chi}_q^0(\omega) = -\frac{1}{N} \sum_k \begin{pmatrix} 1 & \varepsilon_k + \varepsilon_{k+q} \\ \varepsilon_k + \varepsilon_{k+q} & (\varepsilon_k + \varepsilon_{k+q})^2 \end{pmatrix} \times \left[\frac{n_{k+q,\uparrow}(1-n_{k,\downarrow})}{\omega + \varepsilon_{k+q} - \varepsilon_k + i\delta} - \frac{n_{k,\downarrow}(1-n_{k+q,\uparrow})}{\omega + \varepsilon_{k+q} - \varepsilon_k - i\delta} \right]. \tag{50}$$

The RPA series for the spin excitations then corresponds to the following Dyson equation:

$$\boldsymbol{\chi}_q(\omega) = \boldsymbol{\chi}_q^0(\omega) - \boldsymbol{\chi}_q^0(\omega) \mathbf{M}_q \boldsymbol{\chi}_q(\omega), \tag{51}$$

with the interaction kernel

$$\mathbf{M}_q = \begin{pmatrix} N_q & \frac{z'}{z_0} \\ \frac{z'}{z_0} & 0 \end{pmatrix}. \tag{52}$$

As a check of the consistency of our approach, we determine the paramagnetic-ferromagnetic and paramagnetic-antiferromagnetic phase boundaries. This can be compared with previous results within the GA obtained by evaluating the vanishing of the corresponding order parameter. In case of the ferromagnetic instability we have to analyze the limit $\lim_{q\to 0} \boldsymbol{\chi}_q(\omega = 0)$ so that the susceptibility matrix simplifies to

$$\boldsymbol{\chi}_0^0(\omega = 0) = N(\varepsilon_F) \begin{pmatrix} 1 & 2\varepsilon_F \\ 2\varepsilon_F & 4\varepsilon_F^2 \end{pmatrix}, \tag{53}$$

where $N(\varepsilon_F)$ denotes the density of states at the Fermi level ε_F. The inversion of Eq. (51) yields as a condition for the existence of a pole at $\omega = 0$ and $q = 0$

$$\mathrm{Det}[\mathbf{1} + \boldsymbol{\chi}_0^0(\omega = 0)\mathbf{M}_0] \equiv 1 + F_0^a = 0, \tag{54}$$

with the Landau parameter F_0^a:

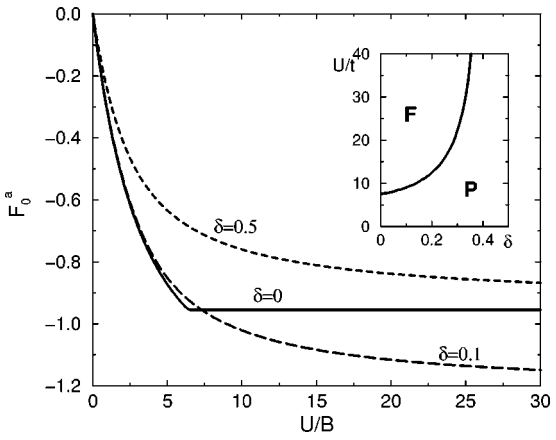

FIG. 1. Landau parameter F_0^a as function of U/B for an infinite-dimensional hypercubic lattice. The inset shows the paramagnetic-ferromagnetic instability line.

$$F_0^a = N(\varepsilon_F)\left[e_0(2z_0 z'' + z'^2) + 4\varepsilon_F \frac{z'}{z_0}\right]. \tag{55}$$

In the half-filled case ($\delta=0$) and a symmetric density of states ($\varepsilon_F=0$) this expression naturally coincides with Vollhardt's result [see Eq. (61) in Ref. 4]. Figure 1 displays F_0^a for a Gaussian density of states

$$N(\omega) = \frac{1}{\sqrt{2\pi}B}\exp\left(-\frac{\omega^2}{2B^2}\right), \tag{56}$$

which corresponds to an infinite-dimensional hypercubic lattice. In this case the GA becomes exact for the energy functional of the Gutzwiller wave function. Due to the occurrence of the Brinkman-Rice transition at half filling F_0^a saturates at a value $F_0^a > -1$ for $U>1$. Thus, in this particular case, there is no second-order paramagnetic-ferromagnetic phase transition. The condition $F_0^a = -1$ can be fulfilled in a restricted doping range, i.e., $0<\delta<0.418$, and the corresponding instability line is shown in the inset of Fig. 1. We find complete agreement of our RPA approach with the phase diagram determined by a variational approach in Ref. 30.

In order to investigate the instability toward antiferromagnetism, we study the $\omega=0$ susceptibility at wave vector $Q=(\pi,\pi,\pi,\ldots)$. The inspection of Eq. (50) reveals that in the case of a nearest-neighbor hopping tight-binding band with $\varepsilon_{k+q}=-\varepsilon_k$ only the (1,1) matrix element of the bare susceptibility is different from zero

$$[\chi_Q^0(\omega=0)]_{11} = \frac{1}{\sqrt{8\pi}B} E_1\left(\frac{1}{2}\frac{\varepsilon_F^2}{B^2}\right), \tag{57}$$

where $E_1(x)$ denotes the exponential integral.[31] The RPA series of Eq. (51) then leads to

$$[\chi_Q(\omega=0)]_{11} = \frac{[\chi_Q^0(\omega=0)]_{11}}{1+N_Q[\chi_Q^0(\omega=0)]_{11}},$$

$$N_Q = e_0\{2z_0 z'' - (z')^2\}. \tag{58}$$

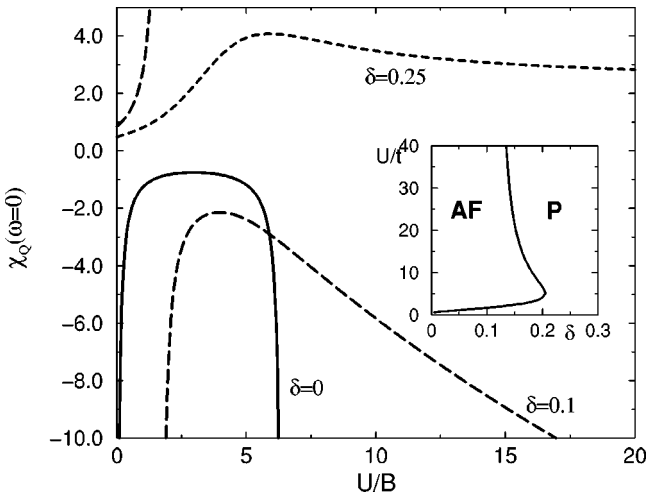

FIG. 2. RPA static susceptibility $[\chi_Q(\omega=0)]_{11}$ as function of U/B for an infinite-dimensional hypercubic lattice. The inset shows the paramagnetic-antiferromagnetic instability line.

We show the behavior of $[\chi_Q^0(\omega=0)]_{11}$ for various δ in Fig. 2.

Due to the complete nesting, the bare susceptibility $[\chi_Q^0(\omega=0)]_{11}$ diverges for $\delta=0$. Hence in this case the singularities of $[\chi_Q(\omega=0)]_{11}$ are determined by the zeros of the interaction kernel N_Q, which naturally vanishes for $U/B=0$ but also at the Brinkman-Rice transition where $z_0 \to 0$. The latter, however, is irrelevant since it occurs in the antiferromagnetic phase. The pole at $U/B=0$ indicates that the instability toward antiferromagnetism at half filling occurs at arbitrarily small interaction also in infinite dimensions. For finite δ the bare magnetic susceptibility is finite and consequently the pole of $\chi_Q(\omega=0)$ is due to the vanishing of the RPA denominator in Eq. (58). It turns out that the static magnetic susceptibility has exactly one pole in the range $0 \leqslant \delta < 0.117$, two poles in the range $0.117 \leqslant \delta < 0.2048$ and no pole for $\delta \geqslant 0.2048$. For completeness, Fig. 2 also displays $\chi_Q(\omega=0)$ for $\delta=0.25$, where there is a small enhancement for those values of U/B where the instability occurred for smaller δ. The inset of Fig. 2 shows the antiferromagnetic-paramagnetic instability line constructed from the poles of $\chi_Q(\omega=0)$. Again we find complete agreement with the variational approach of Ref. 30. Note that one should also determine the first-order boundaries between the ferromagnetic and antiferromagnetic phases. Since our intention is limited to a demonstration of the consistency of the GA+RPA approach, we refer the reader to Ref. 30, where the antiferromagnetic-ferromagnetic phase boundaries have been determined by comparing the respective ground-state energies.

C. Comparison with HF+RPA and exact diagonalization

In the preceding section we have mainly focused on the static limit of our RPA approach. This final part is devoted to an analysis of the magnetic properties of the GA+RPA method, which is compared to the HF+RPA and the exact results on a 4×4 Hubbard cluster with nearest-neighbor

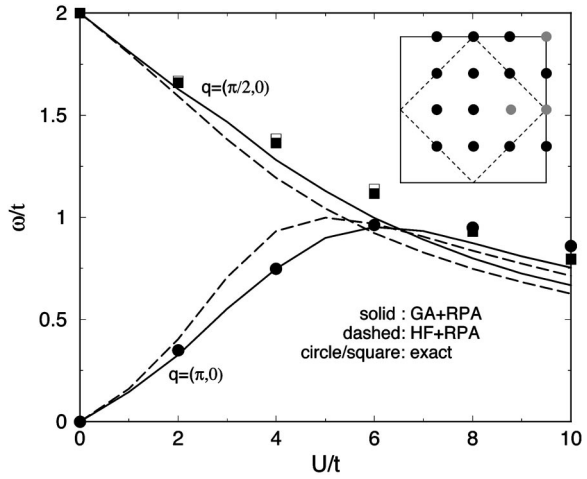

FIG. 3. Magnetic excitations at $q=(\pi/2,0)$ and $q=(\pi,0)$ as a function of U/t for a half-filled 4×4 cluster: GA+RPA (solid line), HF+RPA (dashed line), and exact diagonalization (full circles and full squares). The exact diagonalization results for the excitation at $q=(\pi/2,\pi)$ are also reported (empty squares). In the inset: the q-point mesh of the 4×4 cluster and the dashed square indicates the doubled Brillouin zone. Grey points indicate the important wave vectors of the magnetic excitations.

hopping. For the half-filled system we additionally compare our results with quantum Monte Carlo simulations for the spin-wave velocity.

1. Half-filled system

We start with the half-filled system with eight spin-up and eight spin-down particles. The ground-state Slater determinant for the GA and the HF approximation corresponds to a spin-density wave (SDW), which breaks the spin-rotational symmetry of the Hamiltonian. As a consequence the transverse magnetic excitations contain zero-energy Goldstone modes at wave vector $Q=(\pi,\pi)$. To avoid numerical instabilities, we have added a small perturbation to the Hamiltonian

$$V=\alpha\sum_i (S_i^z)^2, \tag{59}$$

with $\alpha\sim10^{-4}t$, which shifts the Goldstone modes to small but finite energies ($\sim\alpha$). In the exact solution an analog pole appears at small but nonzero frequency ($\omega/t\approx0.145$) due to the finiteness of the cluster. In the thermodynamic limit long-range order is recovered[32] and a Goldstone mode will appear as in the mean-field solution with a weight related to the order parameter. Here, we are interested in the finite-frequency behavior and, therefore, we exclude the exact and approximate ''Goldstone-like'' poles from the comparison and restrict ourselves to the finite-frequency (triplet) excitations, which, for the chosen value of α, do not sensitively depend on the anisotropy field Eq. (59).

Figure 3 shows the magnetic excitation energies as a function of U/t evaluated within the GA+RPA, the HF+RPA and the exact diagonalization. Note that the 4×4 system has a further accidental symmetry, which causes degeneracy between the $q=(\pi/2,\pi/2)$ and $q=(\pi,0)$ excitations. Furthermore, the SDW ground state of the GA and HF solution leads to the doubling of the Brillouin zone (see inset of Fig. 3) so that, besides the antiferromagnetic wave vector Q, only $q=(\pi/2,0)$ and $q=(\pi,0)$ correspond to independent excitations. On the other hand, on the 4×4 lattice, we have that the exact energies at $q=(\pi/2,0)$ and $q=(\pi/2,\pi)$ are slightly different.

The small-U behavior of the lowest excitation energy in Fig. 3 can be well understood from the SDW picture. Within this approximation, the band structure in the reduced Brillouin zone is given by $E_q=\pm\sqrt{\varepsilon_q^2+\Delta^2}$, with $\varepsilon_q=-2t[\cos(q_x)+\cos(q_y)]$ and Δ denotes the SDW gap. Since we study a half-filled system, all states with $E_q<0$ are occupied. Consider first the $q=(\pi,0)$ excitation which can be attributed to a spin-flip transition from $q_1=(-\pi/2,\pm\pi/2)$ to $q_2=(\pi/2,\pm\pi/2)$ so that the excitation energy is given by $\omega=E_{q_1}-E_{q_2}=2\Delta$. The SDW gap in the HF approximation is related to the on-site magnetization $\Delta^{HF}=2U|S_z|$, whereas within the KR formulation of the GA it is determined by the difference in the local spin-dependent Lagrange multipliers $\Delta^{GA}=\lambda_\uparrow-\lambda_\downarrow$. Since in the limit $U\to0$ the GA reduces to the HF approximation, both excitation energies coincide in this regime and also agree with the exact result. On the other hand, for $U/t\gtrsim1$, where RPA corrections become important, it can be seen from Fig. 3 that the GA+RPA is in much better agreement with exact diagonalization than the corresponding HF+RPA result. As a consequence, the GA+RPA gives a quite accurate description of the crossover (at $U/t\approx6$) from the SDW regime, where a gap proportional to U opens along the Fermi surface, to the Heisenberg regime, where there are low-energy magnetic excitations with energy scale t^2/U.

For the higher-energy triplet excitation at $q=(\pi/2,0)$, the GA+RPA yields energies which are slightly lower than the exact result. However, whereas the discrepancy for the GA+RPA at $U/t=6$ is around 10%, the HF+RPA deviates by almost 20% from the exact diagonalization result.

In the Heisenberg regime we thus observe that the magnetic excitations within GA+RPA are shifted to slightly higher energies as compared to HF+RPA. The associated renormalization constant Z_c of the spin wave velocity can be obtained by fitting the k-dependent spin excitations to the dispersion relation $\omega_k=\sqrt{2}c\sqrt{1-\frac{1}{4}[\cos k_x+\cos k_y]}$.[33] The spin-wave velocity extracted for a 8×8 lattice and $U/t=8$ is obtained as $c_{GA}=0.64$ which is in excellent agreement with the estimate from Monte Carlo simulations in Ref. 34.

In order to have information on the accuracy of the GA+RPA for finite frequencies, we report in Fig. 4 the local magnetic susceptibility

$$\chi(\omega)=\sum_q\sum_{m>0}|\langle\Psi_m|S_q^+|\Psi_0\rangle|^2\delta[\omega-(E_m-E_0)], \tag{60}$$

for the GA+RPA and the HF+RPA approximations and the exact diagonalization for $U/t=4$. The δ functions in Eq. (60) have been replaced by Lorentzians with width $0.1t$.

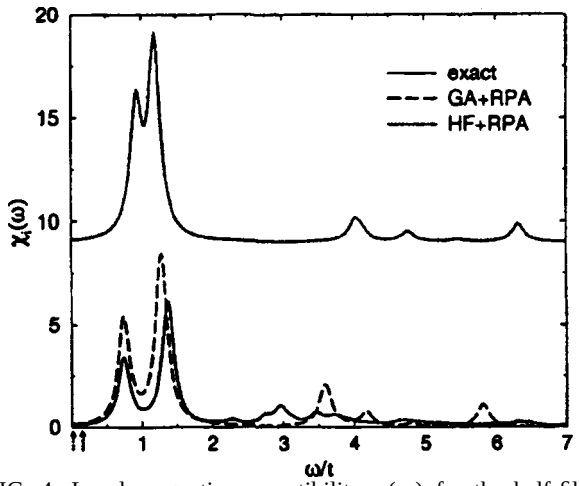

FIG. 4. Local magnetic susceptibility $\chi(\omega)$ for the half-filled 4×4 cluster calculated within exact diagonalization, GA+RPA and HF+RPA for $U/t=4$. The HF+RPA curve has been shifted for convenience. The two arrows indicate the energy of the lowest $Q=(\pi,\pi)$ excitation at $\omega/t\approx0.145$ (exact diagonalization) and $\omega/t=0$ (RPA Goldstone mode).

The two lowest-energy excitations are quite accurate within the GA+RPA approach except for a moderate overestimation of the intensity which becomes much worse in HF+RPA. Interestingly, also the high-energy spin fluctuations are in the correct frequency range.

It should be noted that the spectral weight is constrained by the following sum rule:

$$\int_0^\infty \mathrm{d}\omega\,\omega\chi(\omega) = -\frac{1}{2}\langle T\rangle_{GA}, \tag{61}$$

where $\langle T\rangle_{GA}$ is the average value of the kinetic energy in the GA. The sum rule Eq. (61) relates the RPA correlation function $\chi(\omega)$ to the kinetic energy computed within the GA. A similar sum rule is valid in HF+RPA with the kinetic energy computed in HF. In Ref. 16, we have already demonstrated that the GA kinetic energy is in remarkable agreement with the exact result over a large doping range which in the present context gives additional support to the GA+RPA approach also in the magnetic sector. On the other hand, the HF approximation is of inferior quality in describing excitation energies and the total kinetic energy. Therefore it is not surprising that also spectral weights perform much worse than in the GA+RPA approach.

Finally, Fig. 5 displays the frequency evolution of the first moment of $\chi(\omega)$

$$M^1(\omega) = \int_0^\omega d\tilde{\omega}\,\tilde{\omega}\chi(\tilde{\omega}), \tag{62}$$

for the same parameters as in Fig. 4. Note that $M^1(\omega)$ contains the contribution from the lowest $Q=(\pi,\pi)$ excitations (i.e., the Goldstone modes in the mean-field plus RPA), which appear as the offsets at small energies. From the inset of Fig. 5, it can be seen that, especially at low frequencies, the GA+RPA approach provides a much better approximation for the exact $M^1(\omega)$ than HF+RPA, both with respect

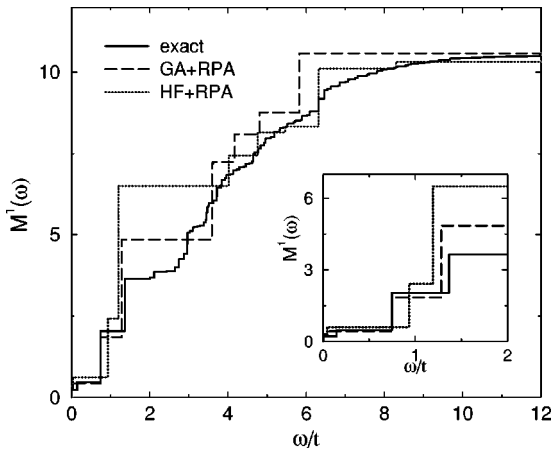

FIG. 5. Cumulative sum of the first moment of $\chi(\omega)$ for the exact result, GA+RPA, and HF+RPA. Data are for a half-filled 4×4 cluster and $U/t=4$. Inset: a detail of the low-energy part.

to the poles and intensities. Both the HF+RPA and the GA+RPA approximate the incoherent part of the exact spectrum (i.e., for $\omega/t>2$) by a rather small set of excitations. However, the corresponding steplike evolution of the first moment of $\chi(\omega)$ is quite close to the exact result.

2. Doped system

We finally investigate a 4×4 cluster with five spin-up and five spin-down particles, corresponding to a closed-shell configuration. The HF solution undergoes a magnetic instability with wave vector $q=(\pi/2,\pi)$ at $U_{crit}/t\approx4.365$, marked by the softening of the corresponding excitation at this critical value. For $U>U_{crit}$ the HF+RPA spectrum has a Goldstone mode and in general the performance is very poor consistently with the fact that a broken symmetry state is not expected even in the thermodynamic limit, therefore, we restrict to the more physical paramagnetic solution. In the GA case the paramagnetic solution can be stabilized for much larger values of U/t providing a reasonable starting point in a broader parameter range just as in the two-site case. The GA+RPA approach captures the behavior of the exact solution (namely, the softening of triplet excitations) at least in a qualitative way, although quantitative deviations increase with increasing U/t (see Fig. 6).

In Fig. 7, we compare the local susceptibility of the HF+RPA, the GA+RPA, and the exact diagonalization for $U/t=4$, i.e., for values of U/t smaller than the magnetic instability. The GA+RPA not only gives a rather good estimate to the lowest excitation energy but in addition provides a good approximation for the corresponding intensity. Note that, since for the given value of U/t the HF solution is already close to the $q=(\pi/2,\pi)$ instability, we observe a strong softening of the lowest-energy excitation resulting in a significantly enhanced oscillator strength.

Finally, we have also evaluated the cumulative integral of the first moment of $\chi(\omega)$ for the GA+RPA and exact diagonalization, which is shown in the inset of Fig. 7. Due to the sum rule Eq. (61) and the excellent kinetic-energy approximation of the GA, the integrated weight of the GA+RPA

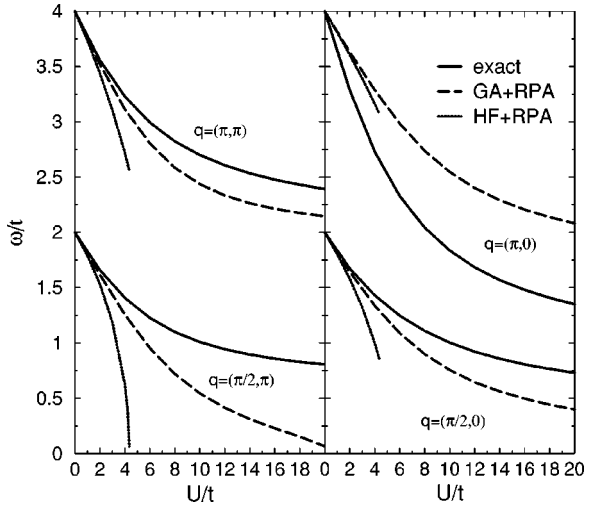

FIG. 6. Magnetic excitations for wave vectors $q=(\pi,\pi)$ and $q=(\pi/2,\pi)$ (left panel) and for $q=(\pi,0)$, $q=(\pi/2,0)$ (right panel) as a function of U/t for the exact diagonalization (solid line), GA + RPA (dashed line), and HF + RPA (dotted line). The HF + RPA are shown for $U<U_{crit}$.

and the exact diagonalization are in excellent agreement. Moreover, we again observe that the GA + RPA provides a rather good steplike approximation to the exact evolution of the spectral weight as a function of the frequency.

IV. CONCLUSION

In this paper, we have presented a detailed investigation of the quality of the GA + RPA approach for the computation of the magnetic excitations. The present computation is complementary to the previous computation in the charge sector.[16,17] An unexpected outcome of the present work is a further justification of the antiadiabatic assumption for the time evolution of the double occupancy, which was needed in the charge but not in the magnetic channel. The fact that the two calculations for the spin and the charge sector give the correct degeneracy of the excitation spectrum for a spin-rotational invariant system (the two-site Hubbard model) clearly indicates that such an assumption was indeed correct, i.e., other possibilities like to keep the double occupancy fixed at the stationary value (rather than to follow the time evolution of the density matrix) would had lead to an unphysical breaking of spin-rotational symmetry.

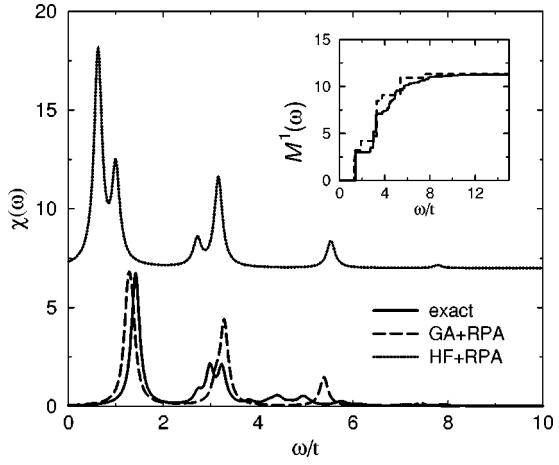

FIG. 7. Local magnetic susceptibility $\chi(\omega)$ for the 4×4 cluster with ten particles calculated within exact diagonalization, GA + RPA and HF + RPA for $U/t=4$. The HF + RPA curve has been shifted for convenience. The inset shows the cumulative sum of the first moment of $\chi(\omega)$ for the exact result and the GA + RPA.

The present formalism is based on a Gutzwiller-type energy functional, which can be either obtained from the spin-rotational invariant KR slave-boson scheme[23] or alternatively from the standard GA with spin-rotated Slater determinants.[24] In our approach, due to the fact that all bosonic fields have been already eliminated from the saddle-point energy functional, it turns out that the evaluation of RPA fluctuations around the GA solution is significantly simplified. In the present paper, we have restricted the calculations of the magnetic excitations to small Hubbard clusters in order to compare with exact diagonalization results. The better performance of GA + RPA with respect to HF + RPA has been demonstrated for both excitation energies and the corresponding intensities. However, compared to numerical methods[35] our approach can be pushed to much larger systems. In particular, it is suitable for the evaluation of magnetic excitations around inhomogeneous solutions of Hubbard-type models, where it is constrained to the same size limitations than the unrestricted HF + RPA approach. This is interesting in connection with the magnetic susceptibility in nickelates and high-T_c cuprates, which are both characterized by the presence of strong electronic correlations and inhomogeneous charge distributions in some part of the phase diagram. Work in this direction is in progress.

ACKNOWLEDGMENTS

G.S. and P.R. gratefully acknowledge financial support from the Deutsche Forschungsgemeinschaft, and F.B. the support from INFM.

APPENDIX A: DERIVATIVES OF THE HOPPING FACTOR

The derivatives appearing in Eqs. (21) and (22) are given by

$$\frac{\partial z_{i,\sigma,-\sigma}}{\partial \rho_{ii}^{-\sigma,\sigma}} = \frac{1}{2}\frac{z_{i\uparrow\uparrow}^0 - z_{i\downarrow\downarrow}^0}{S_i^z}, \tag{A1}$$

$$\frac{\partial^2 z_{i,\sigma\sigma}}{\partial \rho_{ii}^{\sigma,-\sigma}\partial \rho_{ii}^{-\sigma,\sigma}} = \frac{\sigma}{2S_i^z}\left\{ -\frac{z_{i\uparrow\uparrow}^0 - z_{i\downarrow\downarrow}^0}{S_i^z} + \sqrt{\rho_i^{\sigma\sigma}(1-\rho_i^{\sigma\sigma})} \times\left[\frac{\sqrt{1-\rho_{ii}+D_i}}{\sqrt{\rho_i^{\sigma\sigma}-D_i}} - \frac{\sqrt{D_i}}{\sqrt{\rho_i^{-\sigma-\sigma}}}\right] - \frac{1-2\rho_i^{\sigma\sigma}}{\rho_i^{\sigma\sigma}(1-\rho_i^{\sigma\sigma})} z_{i,\sigma\sigma}^0 \right\}. \tag{A2}$$

In case of a homogeneous, paramagnetic saddle point these expressions simplify to

$$\frac{\partial z_{i,\sigma,-\sigma}}{\partial \rho_{ii}^{-\sigma,\sigma}} \equiv z' = \frac{2\delta}{1-\delta^2}\left(\frac{1}{z_0} - z_0\right), \tag{A3}$$

$$\frac{\partial^2 z_{i,\sigma\sigma}}{\partial \rho_{ii}^{\sigma,-\sigma}\partial \rho_{ii}^{-\sigma,\sigma}} \equiv z'' = \frac{2z_0}{(1-\delta^2)^2}\left\{1 - 2\delta^2\left(\frac{1}{z_0^2} - 1\right)\right\} - \frac{1}{2}\frac{z_0}{(1-\delta-2D)^2}, \tag{A4}$$

where z_0 denote the elements of the z matrix defined in Eq. (40).

APPENDIX B: DERIVATION OF THE RPA MATRICES

In order to give explicit expressions for the RPA matrices A and B as defined in Eq. (30) one has to first diagonalize the Gutzwiller Hamiltonian Eq. (19) via

$$c_{i,\sigma} = \sum_{\nu} \Phi_i(\nu,\sigma) a_{\nu,\sigma}, \tag{B1}$$

where ν refers to either particle (p) or hole (h) states. Inserting this transformation in the expansion Eq. (20) leads to the following expressions for A and B:

$$\begin{aligned}
A_{ph,p'h'}^{\sigma\sigma'} &= (\varepsilon_{p\sigma} - \varepsilon_{h,-\sigma})\delta_{pp'}\delta_{hh'}\delta_{\sigma\sigma'} \\
&\quad + \delta_{\sigma\sigma'}\sum_{ij} N_{ij}\Phi_i(p\sigma)\Phi_i(h,-\sigma)\Phi_j(p'\sigma) \\
&\quad \times \Phi_j(h',-\sigma) + R_{ph,p'h'}^{\sigma\sigma'} + R_{p'h',ph}^{-\sigma\sigma'},
\end{aligned}$$

$$\begin{aligned}
B_{ph,p'h'}^{\sigma\sigma'} &= \delta_{\sigma,-\sigma'}\sum_{ij} N_{ij}\Phi_i(p\sigma)\Phi_i(h,-\sigma) \\
&\quad \times \Phi_j(p',-\sigma)\Phi_j(h'\sigma) + T_{ph,p'h'}^{\sigma\sigma'} + T_{p'h',ph}^{\sigma\sigma'},
\end{aligned} \tag{B2}$$

where

$$\begin{aligned}
N_{ij} &= 2\delta_{ij}\sum_{n,\sigma} t_{nj} z_{n,\sigma\sigma}^0 \rho_{nj,\sigma\sigma}^0 \frac{\partial^2 z_{j,\sigma\sigma}}{\partial(\rho_{jj,\uparrow\downarrow})\partial(\rho_{jj,\downarrow\uparrow})} \\
&\quad + t_{ij}\frac{\partial z_{i,\uparrow\downarrow}}{\partial \rho_{i,\downarrow\uparrow}}\frac{\partial z_{j,\downarrow\uparrow}}{\partial \rho_{j,\uparrow\downarrow}}(\rho_{ij,\uparrow\uparrow}^0 + \rho_{ij,\downarrow\downarrow}^0)(1-\delta_{ij}), \\
T_{ph,p'h'}^{\sigma\sigma'} &= \delta_{\sigma\sigma'}\delta_{\sigma\uparrow}\sum_{ij} t_{ij}\frac{\partial z_{j,\downarrow\uparrow}}{\partial \rho_{jj,\uparrow\downarrow}}\Phi_j(p\uparrow)\Phi_j(h\downarrow) \\
&\quad \times [z_{i,\uparrow\uparrow}^0 \Phi_i(p'\uparrow)\Phi_j(h'\downarrow) + z_{i,\downarrow\downarrow}^0 \Phi_j(p'\uparrow)\Phi_i(h'\downarrow)] \\
&\quad + \delta_{\sigma,\sigma'}\delta_{\sigma\downarrow}\sum_{ij} t_{ij}\frac{\partial z_{j,\uparrow\downarrow}}{\partial \rho_{jj,\downarrow\uparrow}}\Phi_j(p\downarrow)\Phi_j(h\uparrow) \\
&\quad \times [z_{i,\uparrow\uparrow}^0 \Phi_j(p'\downarrow)\Phi_i(h'\uparrow) \\
&\quad + z_{i,\downarrow\downarrow}^0 \Phi_i(p'\downarrow)\Phi_j(h'\uparrow)], \\
R_{ph,p'h'}^{\sigma\sigma'} &= \delta_{\sigma,-\sigma'}\delta_{\sigma\uparrow}\sum_{ij} t_{ij}\frac{\partial z_{j,\downarrow\uparrow}}{\partial \rho_{jj,\uparrow\downarrow}}\Phi_j(p\uparrow)\Phi_j(h\downarrow) \\
&\quad \times [z_{i,\uparrow\uparrow}^0 \Phi_i(h'\uparrow)\Phi_j(p'\downarrow) + z_{i,\downarrow\downarrow}^0 \Phi_j(h'\uparrow)\Phi_i(p'\downarrow)] \\
&\quad + \delta_{\sigma,-\sigma'}\delta_{\sigma\downarrow}\sum_{ij} t_{ij}\frac{\partial z_{j,\uparrow\downarrow}}{\partial \rho_{jj,\downarrow\uparrow}}\Phi_j(p\downarrow)\Phi_j(h\uparrow) \\
&\quad \times [z_{i,\uparrow\uparrow}^0 \Phi_i(p'\uparrow)\Phi_j(h'\downarrow) \\
&\quad + z_{i,\downarrow\downarrow}^0 \Phi_j(p'\uparrow)\Phi_i(h'\downarrow)].
\end{aligned} \tag{B3}$$

[1] M.C. Gutzwiller, Phys. Rev. Lett. **10**, 159 (1963).
[2] M.C. Gutzwiller, Phys. Rev. **134**, A923 (1964); **137**, A1726 (1965).
[3] W. Metzner and D. Vollhardt, Phys. Rev. Lett. **59**, 121 (1987); Phys. Rev. B **37**, 7382 (1988).
[4] D. Vollhardt, Rev. Mod. Phys. **56**, 99 (1984).
[5] G. Seibold, C. Castellani, C. Di Castro, and M. Grilli, Phys. Rev. B **58**, 13 506 (1998).
[6] J. Lorenzana and G. Seibold, Phys. Rev. Lett. **89**, 136401 (2002).
[7] F. Gebhard, Phys. Rev. B **41**, 9452 (1990).
[8] C. Attaccalite and M. Fabrizio, Phys. Rev. B **68**, 155117 (2003).
[9] G. Kotliar and A.E. Ruckenstein, Phys. Rev. Lett. **57**, 1362 (1986).
[10] E. Arrigoni and G.C. Strinati, Phys. Rev. Lett. **71**, 3178 (1993); Phys. Rev. B **52**, 2428 (1995).
[11] M. Lavagna, Phys. Rev. B **41**, 142 (1990).
[12] J.W. Rasul and T. Li, J. Phys. C **21**, 5119 (1988).
[13] R. Raimondi and C. Castellani, Phys. Rev. B **48**, R11 453 (1993).
[14] R. Raimondi, Phys. Rev. B **51**, 10 154 (1995).
[15] R. Raimondi (private communication).
[16] G. Seibold and J. Lorenzana, Phys. Rev. Lett. **86**, 2605 (2001).
[17] G. Seibold, F. Becca, and J. Lorenzana, Phys. Rev. B **67**, 085108 (2003).
[18] D.J. Thouless, Nucl. Phys. **22**, 78 (1961).
[19] K. Yonemitsu, I. Batistić, and A.R. Bishop, Phys. Rev. B **44**, 2652 (1991); K. Yonemitsu, A.R. Bishop, and J. Lorenzana, *ibid.* **47**, 12 059 (1993).
[20] J. Lorenzana and G. Seibold, Phys. Rev. Lett. **90**, 066404 (2003).
[21] J. Bünemann, J. Phys.: Condens. Matter **13**, 5321 (2001).
[22] W. Zimmermann, R. Frésard, and P. Wölfle, Phys. Rev. B **56**, 10 097 (1997).
[23] T. Li, P. Wölfle, and P.J. Hirschfeld, Phys. Rev. B **40**, 6817 (1989); R. Frésard and P. Wölfle, Int. J. Mod. Phys. B **6**, 237 (1992).
[24] M. Bak and R. Micnas, J. Phys.: Condens. Matter **10**, 9029 (1998).

[25] G. Seibold, E. Sigmund, and V. Hizhnyakov, Phys. Rev. B **57**, 6937 (1998).
[26] G. Seibold, Phys. Rev. B **58**, 15 520 (1998).
[27] P. Ring and P. Schuck, *The Nuclear Many-body Problem* (Springer-Verlag, New York, 1980).
[28] J. Blaizot, G. Ripka *Quantum Theory of Finite Systems* (MIT Press, Cambridge, 1986).
[29] For Hubbard clusters with broken symmetry typical system sizes are $\sim$100–200 lattice sites. For periodic solutions the formalism can be also applied in momentum space with the standard Green function approach (as in Sec. III B), which allows us to treat infinite systems.
[30] P. Fazekas, B. Menge, and E. Müller-Hartmann, Z. Phys. B: Condens. Matter **78**, 69 (1990).
[31] *Handbook of Mathematical Functions*, edited by M. Abramowitz and I. A. Stegun (Dover, New York, 1965).
[32] J.E. Hirsch, Phys. Rev. B **31**, 4403 (1985); S.R. White, D.J. Scalapino, R.L. Sugar, E.Y. Loh, J.E. Gubernatis, and R.T. Scalettar, *ibid.* **40**, 506 (1989).
[33] E. Manousakis, Rev. Mod. Phys. **63**, 1 (1991).
[34] J.E. Hirsch and S. Tang, Phys. Rev. Lett. **62**, 591 (1989).
[35] E. Dagotto, Rev. Mod. Phys. **66**, 763 (1994).